



40 years High Arctic climatological dataset of the Polish Polar Station Hornsund (SW Spitsbergen, Svalbard)

Tomasz Wawrzyniak, Marzena Osuch

Institute of Geophysics, Polish Academy of Sciences, Warsaw, Poland

Correspondence to: Tomasz Wawrzyniak (tomasz@igf.edu.pl)

Abstract. The article presents the climatological dataset from the Polish Polar Station Hornsund located in the SW part of Spitsbergen - the biggest island of the Svalbard Archipelago. Due to a general lack of long-term in situ measurements and observations, the high Arctic remains one of the largest climate-data deficient regions on the Earth, so described series is of unique value. To draw conclusions on the climatic changes in the Arctic, it is necessary to analyse the long-term series of continuous, systematic, in situ observations from different locations and comparing the corresponding data, rather than rely on the climatic simulations only. In recent decades, rapid environmental changes occurring in the Atlantic sector of the Arctic are reflected in the data series collected by the operational monitoring conducted at the Hornsund Station. We demonstrate the results of the 40 years-long series of observations. Climatological mean values or totals are given, and we also examined the variability of meteorological variables at monthly and annual scale using the modified Mann-Kendall test for trend and Sen's method. The relevant daily, monthly, and annual data are provided on the PANGAEA repository (<https://doi.pangaea.de/10.1594/PANGAEA.909042>, Wawrzyniak and Osuch, 2019).

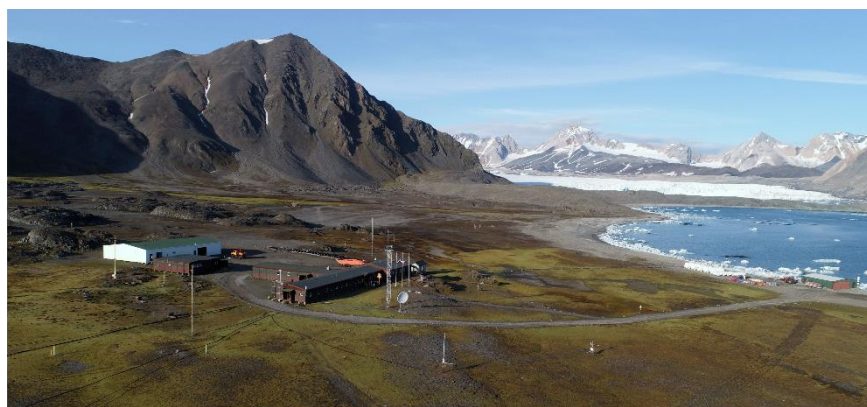
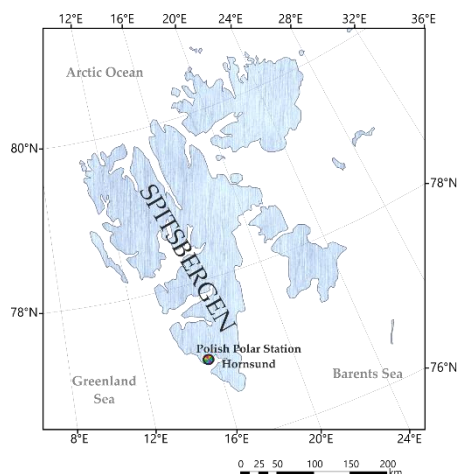
1 Introduction

If the Arctic climate changes are considered, then the long term operational monitoring of meteorological variables including reliable observations and measurements is obligatory. Weather conditions are crucial drivers that have feedback on many environmental components, and it is crucial to have a relevant dataset of atmospheric observation data if analysing the variability and fluctuations of climate at any given location. Climate change in the Arctic reflects a global warming trend, but there are regional differences throughout the area. The climatic characteristics are primarily determined by astronomical factors, but there are differences in the mechanisms that cause a regional warming trend and determine their magnitude. The presence of solar radiation, modified by the degree of cloudiness and type of clouds is the main factor influencing the transfer of energy. During the polar night, the sole source of energy is the dynamic advection of heat from the ocean and atmospheric circulations. The growing number of positive annual air temperature anomalies in the Arctic varies substantially within the



28 region, with the strongest changes observed in the Atlantic sector (Przybylak, 2016). Here, the Greenland Sea to the West of
29 Svalbard is dominated by the West Spitsbergen Current, carrying warm (3–6°C) and salty (>35‰) Atlantic waters towards the
30 Fram Strait. In this region, this flow is over 200 km wide and strongly influences the air temperature in the SW Spitsbergen
31 area, especially during the winter (Walczowski et al., 2017). The specific maritime and mild climatic conditions are also
32 influenced by local and regional factors as the presence of glaciers, orography of the terrain, and location near the seashore.
33 The climatic variables such as air temperature, humidity, and precipitation vary significantly across the archipelago (Nordli et
34 al., 2014; Osuch and Wawrzyniak, 2017a) as well as around the Hornsund Fjord (Araźny et al., 2018). Long-term, high-quality,
35 in-situ consistent meteorological observations have been collected at the Hornsund Station located at the northern shore of this
36 fjord. Relatively to the other parts of the Arctic, air temperatures in Hornsund are the highest at this latitude and their observed
37 changes are the largest on Earth. Recently observed along the western Spitsbergen: higher air temperatures and higher liquid
38 precipitation have many environmental implications, leading to prolongation of the ablation season (Osuch and Wawrzyniak,
39 2017b), negative mass balance of glaciers (Van Pelt et al., 2019), and permafrost degradation (Wawrzyniak et al., 2016).

40 2 Study area



41
42 **Figure 1 Polish Polar Station Hornsund on Spitsbergen**

43 The Stanisław Siedlecki Polish Polar Station in Hornsund (77°00'N 15°33'E) located 300 m from the shore of Isbjørnhamna
44 Bay of the Hornsund Fjord in SW Spitsbergen (Fig. 1), was established during the International Geophysical Year in 1957.
45 Since 1978 it conducts year-round scientific research and is the northernmost permanent Polish scientific site, that throughout
46 the years became a modern interdisciplinary scientific platform that carries out research projects aimed at a better
47 understanding of the functioning of the arctic nature and the changes it undergoes. The Hornsund Fjord is approximately 35
48 km long and approximately 14.5 km wide at its mouth to the Greenland Sea. The coastline of Hornsund is diversified, with
49 multiple bays and glaciated valleys. A recent expansion of the ice-free areas is observed in Svalbard, with the most significant



50 retreats of the tidewater glaciers (Błaszczuk et al., 2013), so the recognition of the changes in the functioning of the
51 environmental system becomes more and more essential. The Station is set on a marine terrace at 10 m a.s.l., covered with sea
52 gravel, raised during Holocene (Lindner et al., 1991), covered by a diversity of tundra vegetation types. The slopes of the
53 nearest mountain ranges Fugleberget (569 m) and Ariekammen (517 m) are located 1 km north from the Station. Around 800
54 m NE from the Station lies the lateral moraine of Hansbreen glacier, which was at its maximum Holocene extent in Little Ice
55 Age (Błaszczuk et al., 2009). Recently the distance from the Station to the front of Hansbreen is around 2.5 km. The ground
56 here has a continuous permafrost layer down to more than 100 m deep (Wawrzyniak et al., 2016).

57 At Hornsund meteorological site indexed by international numbering system 01003 (www.ogimet.com), managed by the
58 Institute of Geophysics Polish Academy of Sciences, since July 1978 year-round, systematic, continuous measurements and
59 observations at WMO standards have been conducted. The results of automatic measurements and visual observations are sent
60 as the SYNOP-code to WMO database every 60 minutes and 3 hours, respectively. Since January 2001 most of the traditional
61 instruments were replaced by an automatic weather station with Vaisala QLC-50 logger. The sensors of the new system have
62 been installed on meteorological mast, situated 160 m SW of the main Station building. In July 2009 Norwegian
63 Meteorological Institute installed an automatic Vaisala weather station that is operating simultaneously at the same mast. In
64 September 2016 Vaisala QLC-50 was replaced by Vaisala MAWS 301. A comprehensive description of measurements and
65 instruments can be found in collective work edited by Marsz and Styszyńska (2013) and in **Table 1**. Although the time series
66 of the data stretches up to July 1978, here we analyse the variability of climatic conditions over the period 1979–2018 and in
67 some cases 1983–2018, based on the availability of observations without gaps. The daily, monthly, and annual averages or
68 sums and the extreme range (min and max), computed from observations are provided in PANGAEA repository (Wawrzyniak
69 and Osuch, 2019).

70 **3 Meteorological variables**

71 Inter-seasonal weather fluctuations are determined by the changing Arctic climate system and atmospheric circulation. The
72 changing global climate also modifies regional conditions. Weather conditions are crucial factors that have local feedback on
73 many environmental components. Meteorological variables collected at the Hornsund Station help to characterise the climate
74 variability in this part of the Arctic and for a long time have been the background for multiple studies conducted in the SW
75 Spitsbergen (Osuch and Wawrzyniak, 2017b, Wawrzyniak et al. 2017). Due to the diurnal variability of all meteorological
76 variables, in this study, we use descriptive statistic methods to present the course and variation of multiple parameters. For
77 most meteorological parameters, monthly mean values are calculated from daily mean values which are retrieved using the 3-
78 hourly values (eight values a day, between 00:00 and 21:00 UTC); in case of precipitation 6-hourly values (12:00, 18:00, and
79 00:00, 06:00 UTC of the following day); and daily sum of total solar radiation from Campbell–Stokes recorder obtained at the
80 midnight.

81



82 **Table 1 Meteorological data measured at Hornsund including variables, current sensors, the period of operation, height, units, and**
 83 **their annual averages or sums.**

Variable	Location	Sensor	Period of operation	Height	Unit	Mean/sum
Air temperature (TA)	77°00'1.261" N 15°32'12.267" E	A traditional thermometer in Stevensons screen, Vaisala HMP 45D, HMP155	1979-2018	2 m agl	[°C]	TAm _{ax} =-1.3 TAm _{ean} =-3.7 TAm _{in} =-6.0
Relative humidity (RH)	77°00'1.261" N 15°32'12.267" E	Hygrometer HMP45D	1979-2018 with gap 01.07.1982-16.08.1982	2 m agl	[%]	79.7%
Precipitation	77°00'5.734" N 15°32'17.077" E	Hellmann Rain Gauge	1979-2018	1 m agl	[mm]	478 mm
Atmospheric pressure (PA)	77°00'1.261" N 15°32'12.267" E	PTB200A	1983-2018	Reduced to the sea level	[hPa]	1008.7 hPa
Wind speed (WS) and direction (WD)	77°00'1.261" N 15°32'12.267" E	Fuess 90z wind meter Vaisala WAA151 Vaisala WMT702	1983-2000 2001-2016 2017-2018	10 m agl	[m/s]	5.5
Sunshine duration (SD)	77°00'5.935" N 15°32'14.3" E	Campbell–Stokes Heliograph	1979-2018	2 m agl	[h]	1030.8
Cloudiness	On location	Visual observations	1983-2018		[octas]	5.85



Visibility	On location	Visual observations	1983-2018		[marine scale]	7.40
------------	-------------	---------------------	-----------	--	----------------	------

84 **3.1 Air temperature**

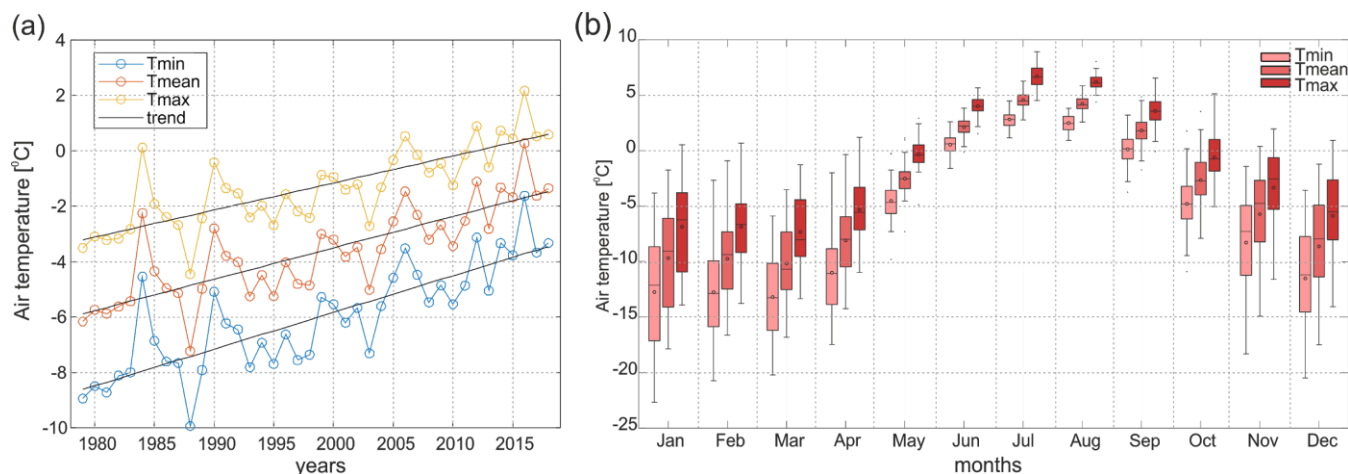
85 Air temperature (TA) can be presumed to be one of the most sensitive indicators of climatic changes. The time series of daily
 86 TA from the Hornsund Station covers the period 1979 to 2018. In the case of daily mean TA, there are no gaps in data while
 87 for maximum and minimum daily TA data for 01.09.1979, 29.02.1980, 15.06.2012, and 19.06.2017 are missing. Figure 2a
 88 presents the variability of the annual mean of minimum, mean, and maximum TA in 1979-2018 at the Hornsund Station. An
 89 upward trend is clearly visible for the three analysed variables. The significance of the trend was estimated by the modified
 90 Mann-Kendall test (Mann, 1945; Kendall, 1975; Hamed and Rao, 1998) taking into account autocorrelation of time series. The
 91 slope of the trend was estimated using Sen's method (Sen, 1968), where the slope is calculated as a median of the slopes of all
 92 pairs of points. The outcomes of the modified Mann-Kendall indicated that the trends are statistically significant; the estimated
 93 p-value is very small (less than $1e-07$) for three presented variables. The estimated slope of trend equal to 1.34, 1.14, and
 94 $1.00^{\circ}\text{C}/\text{decade}$ for minimum, mean, and maximum TA respectively. These are the highest increases of TA on the planet, and
 95 the rest of the world is not expected to experience such changes until the end of this century (Hanssen-Bauer et al. 2019).
 96 The results of trend analyses for mean monthly TA (min, mean, and max) are presented in **Table 2**. In almost all months there
 97 are statistically significant trends except March. In all analysed cases the estimated slope of trend has positive values and
 98 indicated the increase in TA. A comparison of the results between variables shows that the largest changes were found for
 99 minimum daily TA ($1.34^{\circ}\text{C}/\text{decade}$) while the lowest for the maximum daily TA ($1.0^{\circ}\text{C}/\text{decade}$). Taking into account changes
 100 between months, the largest changes were estimated for January, February, and December (larger than $2.0^{\circ}\text{C}/\text{decade}$ for
 101 minimum and mean daily TA). The smallest statistically significant are trends in July and August with slopes of the trend
 102 around $0.3^{\circ}\text{C}/\text{decade}$.

103 Figure 2b shows the boxplots of monthly averages of minimum, mean and maximum daily TA from the period 1979-2018.
 104 The variability of TA depends on the season, with the highest amplitudes during winter months. Summer TA is rather constant,
 105 with monthly means reaching usually slightly below 5.0°C . Average monthly TA during winter and early spring usually drop
 106 below -10.0°C . The results are in general accordance with observations made at other arctic stations and reveal that winter is
 107 characterised by the highest variability of TA. The amplitude between the extreme high and low in this season may be several
 108 times higher than in summer. These fluctuations are determined by the relatively stable anticyclonic subsidence with extreme
 109 cold and the turbulent cyclonic disturbances that bring higher temperatures, greater cloudiness, and heavy precipitation. The
 110 lowest recorded TA measured at a 2 m height above solid ground at Hornsund Station was -35.9°C on 16.01.1981, while the
 111 absolute maximum 15.6°C on 31.07.2015. Mean annual air temperature (MAAT) in long-term 1979-2018 is -3.7°C . The
 112 average coldest month is March with mean TA -10.2°C , and on the average warmest month is July with the mean TA of 4.6°C .



113 The coldest month on record with mean -17.9°C was January 1981, and the warmest June 2016 with mean 6.3°C . Additionally,
 114 in the data set we also provided monthly and annual positive (PDD) and negative degree days (NDD), calculated as the sum
 115 total of daily mean temperatures above or below the 0°C respectively.

116



117

118 **Figure 2 (a) Variability of an annual mean of min, mean, and max air temperatures in 1979-2018. (b) Variability of the monthly**
 119 **mean of min, mean, and max air temperatures in 1979-2018. On each box, the central line indicates the median, the circle represents**
 120 **the mean, and the bottom and top edges of the box indicate the 25th and 75th percentiles, respectively. The whiskers extend to the**
 121 **most extreme data points not considered as outliers, and the outliers are plotted individually as dots.**

122 **Table 2 The slope of the trend in monthly and annual data estimated by Sen’s method in the period 1979-2018 for air temperature**
 123 **and sunshine duration and in 1983-2018 for other variables. The results of trend analysis by modified Mann-Kendall method to**
 124 **account for autocorrelation in the time series. * denotes lack of statistically significant trend at the 0.05 level.**

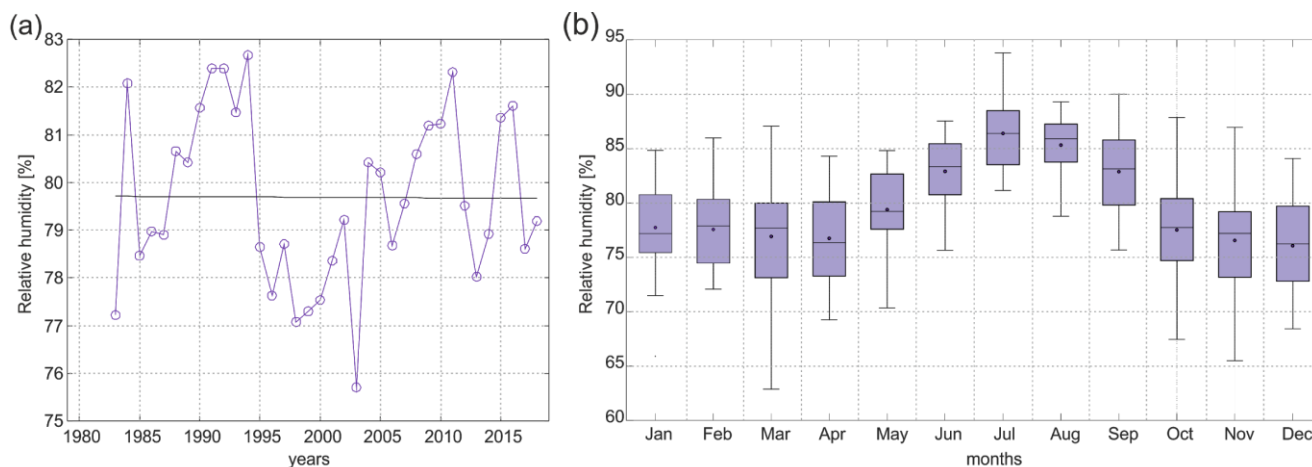
month	T Amin [$^{\circ}\text{C}/\text{dec}$]	T Amean [$^{\circ}\text{C}/\text{dec}$]	T Amax [$^{\circ}\text{C}/\text{dec}$]	RH [%/dec]	Precip [mm/dec]	PA [hPa/dec]	WS [m//decs]	SD [h/dec]	Cloudine ss [octas/d ec]	VV [- /dec]
JAN	2.70	2.29	1.86	-0.33*	3.51	1.54	-0.14*	0.00*	0.12*	- 0.03*
FEB	2.46	2.14	1.74	-0.41*	1.48*	0.50	0.06*	1.38	-0.01*	- 0.06*
MAR	0.74*	0.57*	0.34	-1.13	-1.61*	-0.27	-0.13*	5.52*	0.04*	0.15
APR	1.37	1.00	0.79	-0.64*	-0.41*	-0.66	-0.12*	2.36*	0.16*	0.11*
MAY	0.97	0.70	0.49	-0.27*	1.92*	-0.10	0.40	-10.07*	0.00*	- 0.06*
JUN	0.61	0.52	0.54	-0.65	-3.23*	0.27	0.23*	-1.80*	0.11*	0.13*



JUL	0.36	0.27	0.31	0.26*	1.11*	0.67	0.12*	-5.92*	0.12*	- 0.07*
AUG	0.37	0.33	0.33	0.00*	7.49*	0.30	0.09*	5.18*	0.02*	- 0.02*
SEP	0.73	0.67	0.62	0.62*	19.67	0.18	0.50	-1.33*	0.16*	- 0.10*
OCT	1.16	1.07	1.01	1.50	13.53	1.15	0.05*	0.79*	0.28*	- 0.08*
NOV	1.73	1.46	1.37	0.30*	5.43*	-0.60	0.24*	0.00*	0.26	-0.17
DEC	2.56	2.39	2.18	0.18*	5.24*	-0.95	-0.06*	0.00*	0.13	- 0.10*
annual	1.34	1.14	1.00	0.10*	61.60	0.25	0.08*	-8.39*	0.12	- 0.02*

125 3.2 Air humidity

126 The water vapour drives multiple atmospheric processes and has a significant influence on the global climate. It is the main
 127 greenhouse gas, affecting surface by feedback cycle through changing energy balance through radiative fluxes and cloud
 128 formation. According to general concepts, the Arctic warming of recent decades is accompanied by the hydrological cycle
 129 intensification (Vihma et al., 2015). To understand the variability of water vapour concentration and its causes is highly
 130 important, especially for climate studies as well as in water balance calculations. At the Hornsund Station, the air humidity is
 131 measured recently by sensor HMP155 that replaced the previously used HMP45D sensor. The observations cover period 1979-
 132 2018, but measurements were performed four times a day (0, 6, 12, 18 UTC) within the periods: 1.07.1978-26.07.1981 and
 133 16.08.1982-31.07.1986, two times a day (6 and 18 UTC) from 27.07.1981 to 30.06.1982, eight times a day (0, 3, 6, 9, 12, 15,
 134 18, 21 UTC) since 1.08.1986. Daily time series of the relative humidity (RH) was calculated as a mean of all available
 135 measurements within particular day. There is a gap in the measurements from 01.07.1982 to 15.08.1982. Therefore the trend
 136 analyses were performed for the period 1983-2018.



137

138 **Figure 3 (a) Variability of an annual mean of relative humidity in 1983-2018 at Hornsund. (b) Variability of mean monthly relative**
 139 **humidity in 1983-2018 at Hornsund.**

140 The variability of the annual mean RH in the period 1983-2019 is presented in Figure 3a. The average over the period 1983-
 141 2018 is 79.7%. The range of variability is from 75.7% (2003) to 82.7% in 1994. The trend analyses indicated a lack of a
 142 statistically significant trend.

143 The course of the monthly mean RH in the period 1983-2018 is presented in Figure 3b. Higher values of mean RH are observed
 144 in warmer months of the year and lower during winter. Such high values are attributed to continual dominance of marine air
 145 masses. The annual course of the RH is strongly connected with the air temperature and shows typical variability. It generally
 146 increases with warmer air temperatures. However, most of the trends are not statistically significant at the 0.05 level except
 147 March, June, and October.

148 The analyses at daily time scale indicated that drops of RH below 50% are recorded rather sporadically, although these can
 149 occur throughout the year. Such situations are connected with advection of strongly cooled air masses, foehn effects, or
 150 katabatic winds from Hansbreen (Marsz and Styszyńska, 2013). The minimum of observation reached 24% on 15.01.1981.
 151 The maximum of the observed RH is equal to 100%. Such conditions occurred 27 times in the period 1979-2018.

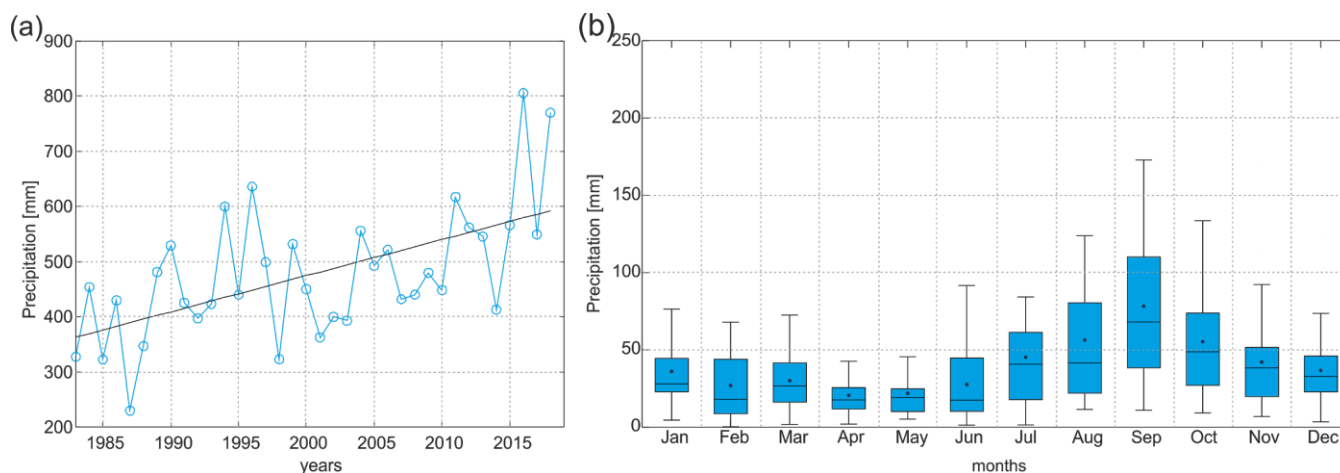
152 3.3 Precipitation

153 In the case of precipitation, the daily sum at the Hornsund Station is calculated from four measurements obtained from
 154 Hellmann Rain Gauge at 12:00, 18:00, and 00:00, 06:00 of the following day, with the orifice 200 cm², placed 1 m above the
 155 ground level. The time series of the daily sum of precipitation cover period 1979-2018 with the gap in July 1982.

156 The influence of the West Spitsbergen Current creates in SW Spitsbergen region a relatively moist climate which is clearly
 157 reflected in the amount of precipitation. In comparison to the other meteorological stations in Spitsbergen (Osuch and
 158 Wawrzyniak, 2017a; Hanssen-Bauer et al. 2019), the annual amount reaching 477 mm is the highest. The variability of the
 159 annual sums of precipitation in the period 1983-2018 is shown in Figure 4a. The amount of precipitation varies from 230 mm



160 in 1987 to 805.5 mm in 2016. The trend analyses indicated large changes, an increase of 61.6 mm/decade for the annual sums
161 of precipitation.

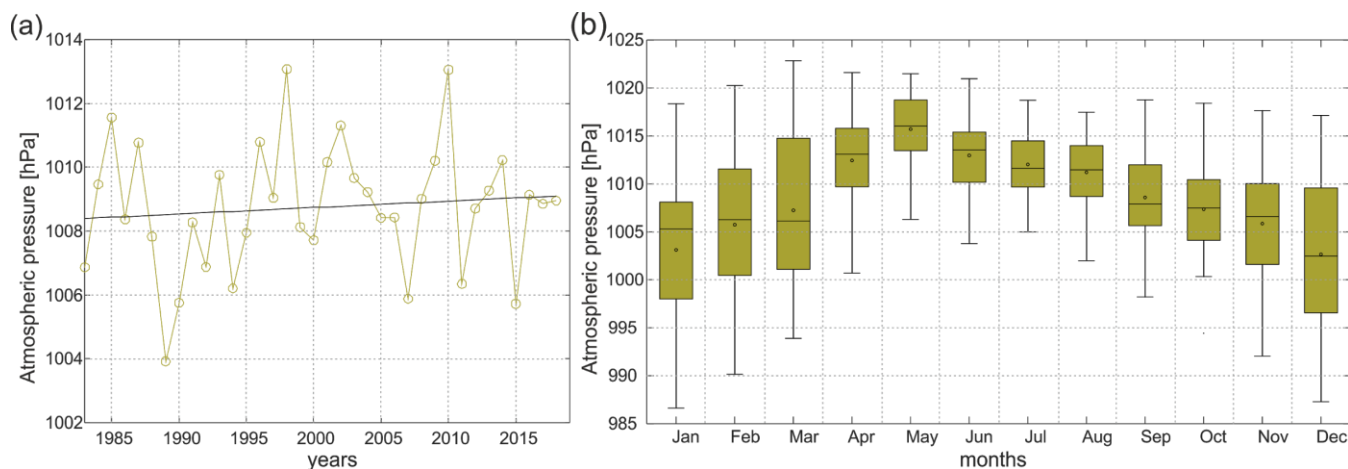


162
163 **Figure 4 (a) Variability of annual sums of precipitation in 1983-2018 at Hornsund. (b) Variability of mean monthly sums of**
164 **precipitation in 1983-2018 at Hornsund.**

165 The annual course of monthly sums of precipitation from the period 1983-2018 is presented in Figure 4b. The driest months
166 are April and May with the average 23 and 24 mm respectively. The highest precipitation is recorded in September reaching
167 on average 75 mm. Trend analyses presented in **Table 2** indicated statistically significant changes in January (3.51
168 mm/decade), September (19.67 mm/decade), and October (13.53 mm/decade).

169 3.4 The atmospheric pressure

170 The measurements of the atmospheric pressure (PA) at Hornsund started in July 1978. In the beginning, PA was measured
171 with a mercury barometer every 3 hours. Since 2001 measurements have been conducted every 60 seconds with a Vaisala
172 PTB200A sensor. The lowest recorded PA reduced to sea level at Hornsund Station was 982.2 hPa on 30.08.1994, while the
173 absolute maximum 1028.5 hPa on 07.08.1987. Mean annual PA in long-term 1983-2018 is 1008.7 hPa and its variability is
174 presented in Figure 5a. It is visible an increasing trend (0.25 hPa /decade) but not statistically significant ($p_{val} > 0.05$).



175

176

177

Figure 5 (a) Variability of mean annual air pressure reduced to sea level in 1983-2018 at Hornsund. (b) Variability of mean annual air pressure reduced to sea level in 1983-2018 at Hornsund.

178

179

180

181

182

183

Figure 5b shows the variability of the mean monthly PA over period 1983-2018. Well pronounced seasonality is visible, with mean monthly pressure higher than 1010 hPa from April to August. The month with the lowest mean PA is December with mean 1002.7 hPa, and the month with the largest PA is May with the mean of 1015.7 hPa. The variability of mean monthly PA within the observation period also is visible with the largest variability in January and February (larger than 30 hPa) and the smallest in July (13.7 hPa). The trend analyses of mean monthly PA resulted in a lack of statistically significant trend for all months.

184

3.5 Wind speed and direction

185

186

187

188

189

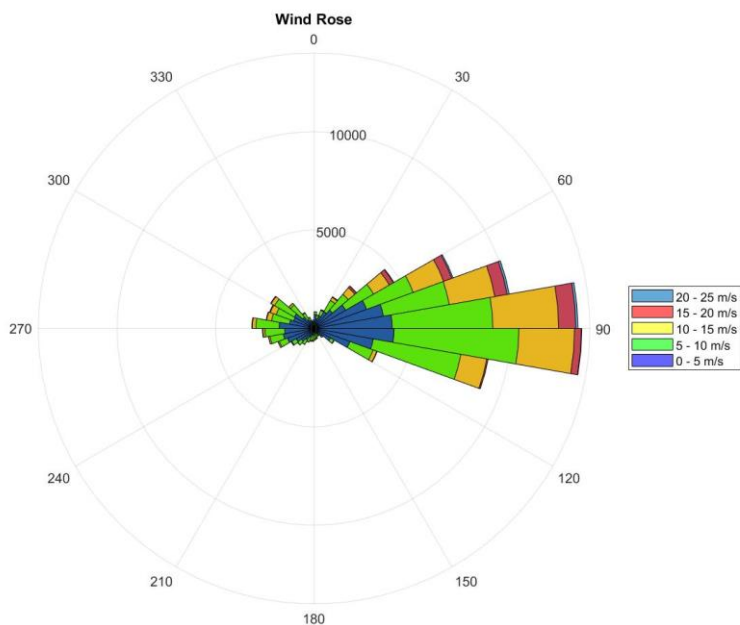
190

191

The wind is a result of atmospheric circulation and is highly correlated with the intensity of cyclonic activity (Przybylak 2016). The wind regime results from the latitudinal shape of the Hornsund fjord, location near the seashore and local topography. The measurements of wind speed (WS) and wind direction (WD) were performed at Hornsund with different sensors: 1978-2000 with the Fuesz 90z wind meter, 2001-2016 with Vaisala WAA151 for direction and wind speed, since 2017 with Ultrasonic Wind Sensor WMT702. At Hornsund Station the height of the anemometer is 10 m above the ground, around 20 m above sea level. WS is measured with an accuracy of 0.1 m/s and WD with 5°. The wind rose for the Hornsund station is presented in Figure 6. Winds blowing from the East, along the fjord, are prevailing.



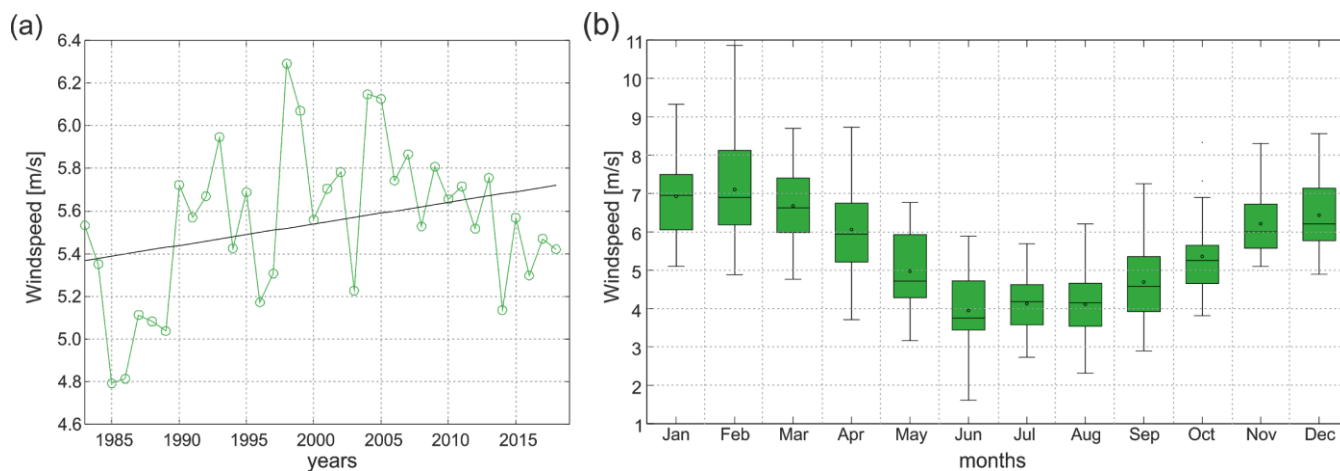
192



193

194 **Figure 6** The wind rose for the Hornsund station for the period 1983-2018.

195 The variability of the mean annual WS at Hornsund in the period 1983-2018 is shown in Figure 7a. The average over the
196 period 1983-2018 is equal to 5.5 m/s. The lowest values of WS was observed in 1985 (4.8 m/s) while the largest in 1998 (6.3
197 m/s). There is a lack of a statistically significant trend in mean annual WS.



198

199 **Figure 7** (a) Variability of mean annual wind speed in 1983-2018 at Hornsund. (b) Variability of the mean monthly wind speed at
200 Hornsund in the period 1983-2018.



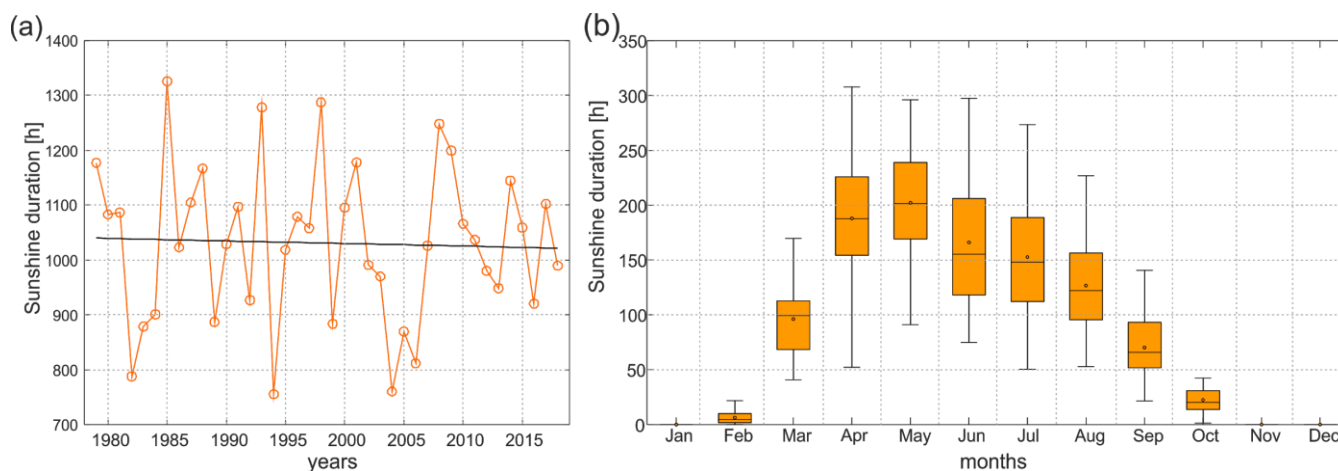
201 The variability of mean monthly WS in the period 1983-2018 is presented in Figure 7b. WS regime is well visible with smaller
 202 average values during summer months (minimum 4.0 m/s in June) and larger average values during winter (maximum 7.1 m/s
 203 in February). Such variability is a result of the extreme cyclone events that often occur during arctic winters (Rinke et al. 2017).

204 **3.6 Sunshine duration**

205 Sunshine duration (SD) is an important meteorological variable that allows the analysis of the atmospheric energy balance
 206 widely used in climate research. Daily SD is measured at Hornsund using a Campbell-Stokes sunshine recorder (CS). It uses
 207 a direct optical method with the heat energy of the Sun's direct radiation burning the card. Such traditional sunshine recorder
 208 has been in service worldwide since the nineteenth century and although there are multiple automatic radiometers used
 209 simultaneously at the Hornsund Station, the longest data is recorded by CS. The time series of sunshine duration cover period
 210 1983-2018. At the Hornsund Station, the polar night lasts 104 days (October 31 – February 11), while the polar day lasts 117
 211 days (April 24 – August 18).

212 Figure 8a shows the variability of the annual sums of SD at Hornsund in the period 1979-2018. The mean value is 1030.8 h
 213 that is about 28% of the potential SD calculated for the Station (Wojkowski et al. 2015). The large span in the annual SD is
 214 visible. The minimum value (755.4 h) was observed in 1994 and maximum (1325.6 h) in 1985. The slightly decreasing trend
 215 in SD is visible but not statistically significant at the 0.05 level.

216



217

218 **Figure 8 (a) Variability of mean annual sunshine duration in 1979-2018 at Hornsund. (b) Variability of the monthly sums of sunshine**
 219 **duration at Hornsund in the period 1979-2018.**

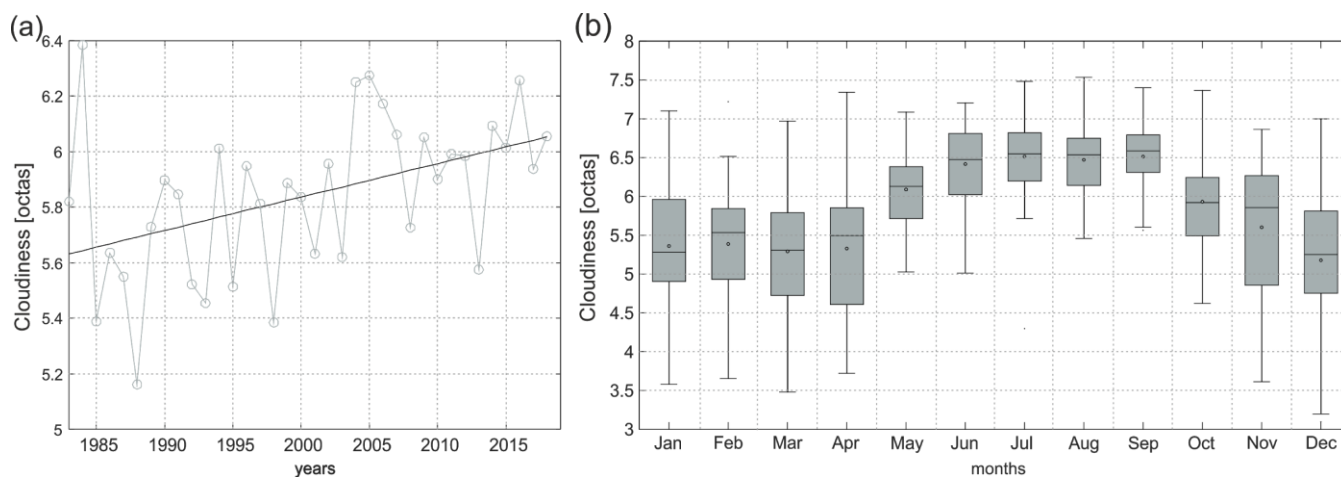
220 Monthly total SD is presented in Figure 8b. Its variability results from the different duration of the day at the location (latitude
 221 77N) with zero SD during the polar night.



222 **3.7 Cloudiness**

223 Arctic clouds have a warming effect on the surface during most of the year because their effect of increasing the downward
 224 longwave radiation dominates their effect of reducing the net solar radiation over high-albedo snow and ice surfaces. In
 225 summer, however, clouds typically have a cooling effect on surface types with a lower albedo, such as the open sea, melting
 226 sea ice, and ground (Intrieri et al., 2002; Shupe and Intrieri, 2004). Observations of cloudiness at the Polish Polar Station in
 227 Hornsund are conducted by meteorologists and describe the predominant sky condition based upon octas (eighths) of the sky
 228 covered by opaque (not transparent) clouds. There are many factors that may hinder the heterogeneity and evaluation of
 229 cloudiness, due to the annual change in the meteorological observers and a fact that observers might be subjective, although
 230 are provided with clear observable criteria.

231 Annual averages of cloudiness in the period 1983-2018 is presented in Figure 9a. The mean over this period equals 5.85 octas.
 232 The minimum value of annual was observed in 1988 (5.16 octas) and maximum in 1984 (6.39 octas). An increasing tendency
 233 of mean annual cloudiness is visible. The estimated trend (slope 0.13 octas/decade) is statistically significant at the 0.05 level.



234 **Figure 9 (a) Variability of mean annual cloudiness in 1983-2018 at Hornsund. (b) Variability of the monthly sums of cloudiness at**
 235 **Hornsund in the period 1983-2018.**
 236

237 The variability of the monthly cloudiness in the period 1983-2018 is presented in Figure 9b. The annual run is characterised
 238 by lower mean cloudiness during the cold period from October till April (5.5-6.0 octas), and it is also characterised by larger
 239 inter-annual variability. The period from May till September is on the average more cloudy (6.0-6.7 octas) and inter-annual
 240 variability is lower.

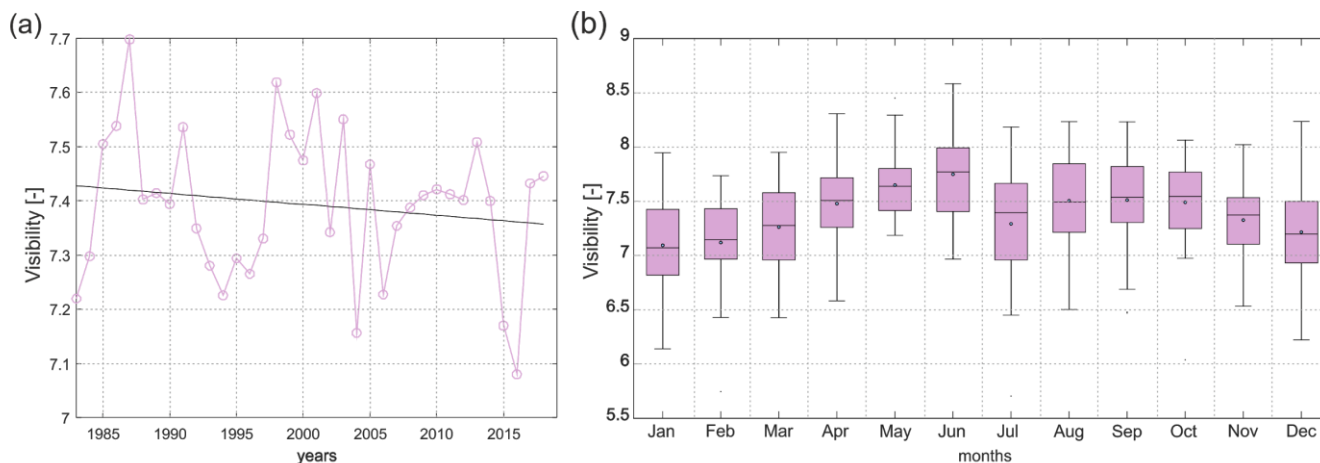
241 **3.7 Visibility**

242 The horizontal visibility is quantified using observations made by meteorologists in the surroundings of the Hornsund Station
 243 with a marine scale that range from 1 to 9. The visual observations are performed using known distances to the surrounding
 244 mountains and other objects. Values 1 and 2 correspond to very bad visibility, 0-50 m and 50-200 m, respectively. Bad



245 visibility (200 m – 1 km) is represented by value 3. Weak horizontal visibility represents conditions with 1-2 km and 2-4 km
 246 that are quantified as 4 and 5 in the applied scale. Moderate horizontal visibility, described as 6 in the scale, represent conditions
 247 when an object or light can be clearly discerned from 4-10 km. Good horizontal visibility (7 in the scale) is 10-20 km, very
 248 good (8) 20-50 km and extremely good (9) is for horizontal visibility larger than 50 km. Noted visibility might be reduced by
 249 multiple factors, including all products of the condensation of water vapour such as fog, precipitation, as well as darkness
 250 during cloudy conditions throughout the polar night, as there are no artificial lights in the area. There are no anthropogenic
 251 factors that would reduce visibility in the vicinity of the Hornsund Station as it is located in the middle of the strictly protected
 252 South Spitsbergen National Park. Due to that reduced visibility cannot be an indicator of poor air quality.

253
 254 Figure 10a shows the variability of mean annual visibility in the period 1983-2018. On average in this period is good horizontal
 255 visibility that amounts 7.40; minimum mean annual visibility was observed in 2016 (7.08) while maximum in 1987 (7.70). A
 256 decreasing tendency is visible (slope of trend -0.02 per decade) however the trend is not statistically significant at the 0.05
 257 level. Variability of the mean monthly visibility at Hornsund in the period 1983-2018 is presented in Figure 10b. It is
 258 characterised by both low inter-annual and interseasonal variability and on average reaches values between 7 and 8.



259
 260 **Figure 10 (a) Variability of mean annual visibility in 1983-2018 at Hornsund. (b) Variability of the mean monthly visibility at**
 261 **Hornsund in the period 1983-2018.**

262 **4 Quality control of the time series**

263 All presented datasets have undergone a thorough quality control process. Such process consisted of multiple steps as the
 264 measurements may not be homogenous due to the varying number of observations during the day, changes of sensors, and
 265 other factors (Estévez et al. 2011). In the first step, the data were visualised as a time series that allowed verification if all data
 266 have been collected and that the record structure is correct, complete, and without any gaps. In this way also the presence of
 267 outliers and step change in the data was tested. In the following step, different variables were compared to test the internal



268 consistency between variables. Such analyses include a comparison of minimum, mean, and maximum daily TA that follow
269 the rule $T_{Amax} > T_{Amean} > T_{Amin}$. In the case of WS and WD following conditions were tested $WS=0$ and $WD=0$, $WS \neq 0$ and
270 $WD \neq 0$. In the third step temporal consistency of time series was analysed with the help of statistical tests of homogeneity
271 (Pettit and Standard Normal Homogeneity Test). In the last step, the same variables but from different meteorological stations
272 in Svalbard were compared. The air temperature time series were tested against observations in Barentsburg, Bjørnøya, Hopen,
273 Longyearbyen (Svalbard Lufthavn), Ny Ålesund, and Sveagruva. For that purpose, the data were visualised and checked with
274 the Standard Normal Homogeneity Test (Alexandersson, 1986; Nordli et al., 1996). The applied algorithm showed good
275 performance in both detecting breakpoints and identifying homogeneous time series. By application of the relative method,
276 with comparison to the other available datasets from Svalbard, the gradual and step changes due to climate change were not
277 found as a source of inhomogeneity.

278 **5 Data availability**

279 The dataset described in this article is available on the PANGAEA repository (Wawrzyniak and Osuch, 2019:
280 <https://doi.pangaea.de/10.1594/PANGAEA.909042>).

281 **6 Summary**

282 This paper has presented details of a long-term (1979–2018) dataset from the meteorological site at the Polish Polar Station
283 Hornsund located in the SW part of Spitsbergen. The data series includes daily, monthly and annual air temperature, PDD,
284 NDD, the sum of precipitation, air humidity, atmospheric pressure, wind speed and direction, sunshine duration, cloudiness,
285 and visibility. This rich dataset, now available online, is a valuable source for documenting the state of the climate in SW
286 Spitsbergen that represents the Atlantic sector of the Arctic. Nowhere on the planet is climate warming faster than here. With
287 the positive trend of mean annual temperature $+1.14^{\circ}\text{C}/\text{decade}$, the climate in Hornsund is warming five times faster than the
288 global average. All climatological variables presented in this study have many environmental implications and there is a broad
289 scientific interest and societal need to understand climate variability and its influence on geoecosystems.

290 **7 Author Contributions**

291 TW and MO wrote the paper and carried out the data processing and analysis.

292 **8 Competing Interests**

293 The authors declare that they have no conflict of interest.



294 Acknowledgements

295 The authors would like to kindly thank the meteorological staff from the Polish Polar Station Hornsund listed here:
296 <https://hornsund.igf.edu.pl/about-the-station/expeditions/> for collecting the data and maintaining the meteorological
297 monitoring. Financial support for this work was provided by the Polish National Science Centre through grant No.
298 2017/27/B/ST10/01269. This work was also partially supported by the Institute of Geophysics, Polish Academy of Sciences
299 within statutory activities No 3841/E-41/S/2019 of the Ministry of Science and Higher Education of Poland.

300 References

- 301 Arażny, A., Przybylak, R., Wszyński, P., Wawrzyniak, T., Nawrot, A., and Budzik, T.: Spatial variations in air temperature
302 and humidity over Hornsund fjord (Spitsbergen) from 1 July 2014 to 30 June 2015, *Geografiska Annaler: Series A, Physical*
303 *Geography*, 100(1), 27-43, doi: 10.1080/04353676.2017.1368832, 2018.
- 304 Błaszczyk, M., Jania, J. A., and Hagen, J.O.: Tidewater glaciers of Svalbard: Recent changes and estimates of calving fluxes,
305 *Polish Polar Research*, 30(2), 85–142, 2009.
- 306 Błaszczyk, M., Jania, J. A., and Kolondra, L.: Fluctuations of tidewater glaciers in Hornsund Fjord (Southern Svalbard) since
307 the beginning of the 20th century, *Polish Polar Research*, 34(4), 327–352, doi:10.2478/popore-2013-0024, 2013.
- 308 Estévez, J., Gavilán, P., and Giráldez, J. V.: Guidelines on validation procedures for meteorological data from automatic
309 weather stations. *Journal of Hydrology*, 402(1-2), 144–154, doi:10.1016/j.jhydrol.2011.02.031, 2011.
- 310 Hamed, K. H., and Rao, R.: A modified Mann-Kendall trend test for autocorrelated data, *J. Hydrol.*, 204, 182–196, 1998.
- 311 Hanssen-Bauer, I., Førland, E.J., Hisdal, H., Mayer, S., Sandø, A.B., Sorteberg, A., Adakudlu, M., Andresen, J., Beldring, S.,
312 Benestad, R., Bilt, W., Bogen, J., Borstad, C., Breili, K., Breivik, Ø., Børsheim, K.Y., Christiansen, H.H., Dobler, A., Engeset,
313 R., Frauenfelder, R., Gerland, S., Gjeltén, H.M., Gundersen, J., Isaksen, K., Jaedicke, C., Kierulf, H., Kohler, J., Li, H., Lutz,
314 J., Melvold, K., Mezghani, A., Nilsen, F., Nilsen, I.B., Nilsen, J.E.Ø., Pavlova, O., Ravndal, O., Risebrobakken, B., Saloranta,
315 T., Sandven, S., Schuler, T.V., Simpson, M.J.R., Skogen, M., Smedsrud, L.H., Sund, M., Vikhamar-Schuler, D., Westermann,
316 S., Wong, W.K.: Climate in Svalbard 2100 – a knowledge base for climate adaptation. Norwegian Centre for Climate Services,
317 Report no. 1/2019, ISSN 2387-3027, 205 pp., 2019.
- 318 Intrieri, J. M., C. W. Fairall, M. D. Shupe, P. O. G. Persson, E. L. Andreas, P. Guest, and Moritz, R. M.: An annual cycle of
319 Arctic surface cloud forcing at SHEBA. *J. Geophys. Res.*, 107, 8039, doi:10.1029/2000JC000439, 2002.
- 320 Kendall, M. G.: Rank Correlation Methods. Charles Griffin: London, 1975.
- 321 Lindner, L., Marks, L., Roszczyńko, W. and Semil, J.: Age of raised marine beaches of northern Hornsund Region, South
322 Spitsbergen, *Pol. Polar Res.*, 12(2), 161-182, 1991.
- 323 Mann, H.: Nonparametric tests against trend, *Econometrica*, 13(3), 245–259, doi:10.2307/1907187, 1945.
- 324 Marsz, A. A., and Styszyńska, A.: Climate and Climate change at Hornsund, Svalbard. Gdynia Maritime University: Gdynia,
325 Poland, ISBN: 978-83-7421-191-8, 2013.



- 326 Nordli, P. Ø., Hanssen-Bauer, I., and Førland, E. J.: Homogeneity Analyses of Temperature and Precipitation Series from
327 Svalbard and Jan Mayen, Norwegian Meteorol. Inst. Report 16/96 KLIMA, 41, 1996.
- 328 Nordli, Ø., Przybylak, R., Ogilvie, A. E. J., and Isaksen, K.: Long-term temperature trends and variability on Spitsbergen: the
329 extended Svalbard Airport temperature series, 1898–2012, *Polar Res.*, 33, 21349, doi: 10.3402/polar.v33.21349, 2014.
- 330 Osuch, M. and Wawrzyniak, T.: Climate projections in the Hornsund area, Southern Spitsbergen, *Pol. Polar Res.*, 37(3), 379–
331 402, doi:10.1515/popore-2016-0020, 2016.
- 332 Osuch, M. and Wawrzyniak, T.: Inter- and intra-annual changes of air temperature and precipitation in western Spitsbergen,
333 *Int. J. Climatol.*, 37, 3082–3097, doi:10.1002/joc.4901, 2017a.
- 334 Osuch, M. and Wawrzyniak, T.: Variations and changes in snow depth at meteorological stations Barentsburg and Hornsund
335 (Spitsbergen), *Ann. Glaciol.*, 58 (75), 11–20, doi:10.1017/aog.2017.20, 2017b.
- 336 Osuch, M., Wawrzyniak, T., and Nawrot, A.: Diagnosis of the hydrology of a small Arctic permafrost catchment using HBV
337 conceptual rainfall-runoff model, *Hydrology Research*, 50(2), 459–478, doi:10.2166/nh.2019.031, 2019.
- 338 Przybylak, R.: *The climate of the Arctic*. 2nd ed. Atmospheric and Oceanographic Sciences Library 52, Heidelberg: Springer;
339 pp. 287, doi:10.1007/978-3-319-21696-6, 2016.
- 340 Rinke, A., Maturilli, R.M. Graham, H. Matthes, D. Handorf, L. Cohen, S.R. Hudson, and Moore, J.C.: Extreme cyclone
341 events in the Arctic: Wintertime variability and trends, *Envir. Res. Lett.*, 12, 094006, doi:10.1088/1748-9326/aa7def, 2017.
- 342 Sen, P. K.: Estimates of the regression coefficient based on Kendall's tau, *Journal of the American Statistical Association*, 63,
343 1379–1389, doi: 10.2307/2285891, 1968.
- 344 Shupe, M. D., and Intrieri, J. M.: Cloud radiative forcing of the Arctic surface: The influence of cloud properties, surface
345 albedo, and solar zenith angle. *J. Climate*, 17, 616–628, doi:10.1175/1520-044, 2004.
- 346 van Pelt, W., Pohjola, V., Pettersson, R., Marchenko, S., Kohler, J., Luks, B., Hagen, J. O., Schuler, T. V., Dunse, T., Noël,
347 B., and Reijmer, C.: A long-term dataset of climatic mass balance, snow conditions, and runoff in Svalbard (1957–2018), *The*
348 *Cryosphere*, 13, 9, 2259–2280, doi: 10.5194/tc-13-2259-2019, 2019.
- 349 Vihma, T., Screen, J., Tjernström, M., Newton, B., Zhang, X., Popova, V., Deser, C., Holland, M., and Prowse, T.: The
350 atmospheric role in the Arctic water cycle: A review on processes, past and future changes, and their impacts, *J. Geophys. Res.*
351 *Biogeosci.*, 121, 586– 620, doi:10.1002/2015JG003132, 2016.
- 352 Walczowski, W., Beszczynska-Möller, A., Wiczorek, P., Merchel, M., and Grynczel, A.: Oceanographic observations in the
353 Nordic Sea and Fram Strait in 2016 under the IO PAN long-term monitoring program AREX, *Oceanologia*, 59(2), 187–194,
354 doi:10.1016/j.oceano.2016.12.003, 2017.
- 355 Wawrzyniak, T., Osuch M., Napiórkowski, J.J., and Westerman, S.: Modelling of the thermal regime of permafrost during
356 1990–2014 in Hornsund, Svalbard. *Polish Polar Research* 37(2): 219–242, doi: 10.1515/popore-2016-0013, 2016.
- 357 Wawrzyniak, T., Osuch, M., Nawrot, A., and Napiórkowski, J.J.: Run-off modelling in an Arctic unglaciated catchment
358 (Fuglebekken, Spitsbergen). *Ann. Glaciol.* 58 (75), 36–46, doi:10.1017/aog.2017.8, 2017.



- 359 Wawrzyniak, T., Osuch, M.: A consistent High Arctic climatological dataset (1979-2018) of the Polish Polar Station Hornsund
360 (SW Spitsbergen, Svalbard). PANGAEA, <https://doi.pangaea.de/10.1594/PANGAEA.909042>, 2019.
- 361 Wojkowski, J., Caputa, Z., and Leszkiewicz, J.: The impact of relief on the diversity of possible sunshine duration at Hornsund
362 region (SW Spitsbergen), *Problemy Klimatologii Polarnej* 25, 179-190, 2015.